




RESEARCH ARTICLE | JUNE 02 2023

Mass spectroscopy of oxygen plasmas with energetic ions

Ruggero Barni ; Matteo Daghetta; Cecilia Piferi ; Claudia Riccardi 



AIP Advances 13, 065207 (2023)

<https://doi.org/10.1063/6.0002313>



25 March 2024 10:29:46



AIP Advances

Special Topic: Field Theory Methods in Condensed Matter Physics for Future Post-Transistor Devices

Submit Today



Mass spectroscopy of oxygen plasmas with energetic ions

Cite as: AIP Advances 13, 065207 (2023); doi: 10.1063/6.0002313

Submitted: 4 April 2023 • Accepted: 18 May 2023 •

Published Online: 2 June 2023



View Online



Export Citation



CrossMark

Ruggero Barni,^{a)}  Matteo Daghetta, Cecilia Piferi,  and Claudia Riccardi 

AFFILIATIONS

Dipartimento di Fisica, Università degli Studi di Milano-Bicocca, P.za della Scienza 3, I-20126 Milano, Italy

^{a)} Author to whom correspondence should be addressed: ruggero.barni@unimib.it

ABSTRACT

An experimental study of the plasma gas phase in low pressure radiofrequency discharges of oxygen is presented. The plasma phase has been studied by means of mass spectroscopy of the neutral and of the charged species, directly sampling the plasma gas phase. We also measured the ion energy distributions. We have studied the influence of the operating conditions on the plasma gas-phase composition. Ion density and energy have been measured as a function of discharge parameters. In particular, we have identified operating conditions in low pressure discharges allowing the extraction of ions from the plasma state with energies exceeding 50 eV. This makes plasma processing with energetic oxygen ions feasible in our device.

© 2023 Author(s). All article content, except where otherwise noted, is licensed under a Creative Commons Attribution (CC BY) license (<http://creativecommons.org/licenses/by/4.0/>). <https://doi.org/10.1063/6.0002313>

I. INTRODUCTION

At present, the preparation of nanostructured materials is of extreme interest for a variety of applications in electronics, energy, and biomedical fields.¹

In different applications, the presence of atomic oxygen is indispensable to support oxidation processes in different application areas, for example, to promote nanostructures on polymer surfaces,² to oxidize organic precursors, useful for creating functional deposits,³ or to break down pollutants, such as Volatile Organic Compounds (VOC).⁴

Recently, air and oxygen plasmas produced in a capacitive reactor have been used to modify the morphology of the material surfaces and have been shown to be effective in the enhancement of the polymeric surface area. The processes responsible for nanostructuring are ascribable to chemical etching on surface polymer promoted by atomic oxygen.² The detection of atomic oxygen is not trivial because of its very high reactivity. Optical diagnostic is not very efficient in that, while mass spectroscopy is able to detect locally the presence of atomic oxygen.

We propose to study the oxygen generation processes in a new configuration based on an inductive plasma characterized by the presence of kinetic ions that could modify the stoichiometry of the chemical reactions increasing the oxygen content. Therefore, our main aim was to identify the operating conditions under which we can control and efficiently generate the atomic oxygen. The analysis

was based on the use of online plasma mass spectrometry, sampling both the neutral and the ionic species produced in the new plasma configuration, with a particular focus on the evaluation of the ionic energies, which could then be involved in the plasma processing of gases or material surfaces.⁵

As a matter of fact, the mass and energy spectra of the oxygen plasma components have been investigated as a function of the gas pressure, flow-rate, radiofrequency (RF) power, and location inside the plasma reactor. Several results have been collected, particularly concerning the ion energy distributions. These have been analyzed in order to extract plasma parameters, such as the average electron energy and the plasma potential.⁶

We also focused on the conditions that allow an energetic and intense flux of oxygen ions to be delivered toward the surface of a material facing the discharge, which could have a distinct role in plasma processing.⁵

II. EXPERIMENTAL

A schematic layout of the set-up is shown in Fig. 1. The plasma source was developed by CCR Technologies GmbH.⁷ It is installed on a Conflat 250 mm flange on the left cap of a cylindrical vacuum chamber (diameter 300 mm, height 200 mm). The electrode consists of a stainless steel curved plate (diameter 170 mm, height 65 mm,

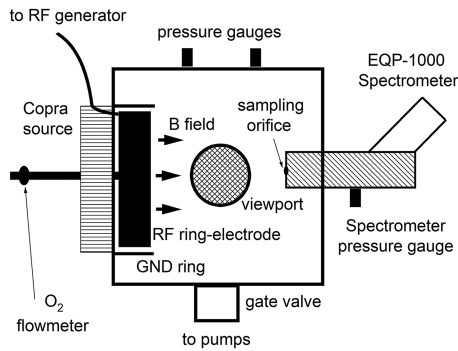


FIG. 1. Lay-out of the experimental setup with the vacuum chamber (diameter 300 mm, length 200 mm) equipped with the RF plasma source (feeding a ring electrode, diameter 170 mm, height 65 mm) and the Hiden EQP-1000 mass spectrometer diagnostics.

thickness 2.5 mm). The configuration is that of a single turn coil fed by an RF wave. The two sides of the plate are connected through two vacuum feedthroughs to the secondary coil of a mutual inductance whose primary coil is driven by the supply RF signal at 13.56 MHz.⁶ Thus, both the current induced in the plate and the voltage supplied to it contribute to the electric field sustaining the discharge. To further enhance the coupling of the electrode, it is possible to tune a static magnetic field B , approximately aligned to the cylinder axis,⁵ which, however, was not employed during the experiments reported here. A couple of variable capacitors in a π configuration allows us to adapt the RF signal, minimizing the reflected power. The vacuum vessel is complemented by a couple of pressure sensors (a full range and 1 mbar capacitive gauge by Pfeiffer) and a micrometer valve and an EL-FLOW flowmeter by BronkHorst to ensure a constant flow of O_2 entering at the center of the left cap. Vacuum is achieved by a turbomolecular (250 L/s by Varian) coupled to a rotary pump (SD2015 by Adixen). To keep the desired pressure there, the effective pumping speed is varied by partially closing a gate valve. Otherwise, direct pumping with the rotary pump (excluding the turbomolecular one) can be performed. On the opposite side of the source, a movable flange connects the chamber to an EQP-1000 ion energy analyzer and quadrupole mass spectrometer by Hiden Ltd.⁸ This device allows us to perform mass spectroscopy of neutral and charged (both positive and negative) species up to 1000 amu. For neutrals, electron impact energies could be varied between 4 and 150 eV, even if the standard energy of 70 eV was used for the data shown here. In particular, abundances and also energy distribution (in a ± 100 eV range) of ions can be measured. Ions and molecules enter the spectrometer through an orifice (100 μm) at the center of the cap of a hollow tube (diameter 50 mm). A dedicated system of electrodes allows us to collect with high efficiency neutral fragments that are ionized along their path or, in alternative, ions that could be selected based on their mass and energy.⁸ As stated above, the orifice can be moved along the cylinder axis scanning up to 300 mm to probe plasma well inside the chamber and the electrode plate.⁹

Apart from the identification of neutral and charged fragments, we focused on the understanding of the energies of ions impinging

on a substrate, which could be directly held on the spectrometer surface or in alternative to it. When the spectrometer is used inside the discharge, a sheath develops between the plasma and the grounded surface surrounding the orifice. Ions have to cross the sheath and their energy spectra are, thus, shifted by a value corresponding to the plasma potential V_p . Besides the shift, the energy spectra $S(E)$ are generally broad^{10,11} and they have been fitted with a general form of energy distribution function f ,¹²

$$S(E) = f(E - q \cdot V_p) = N \cdot \sqrt{(E - q \cdot V_p)} \cdot \exp(-1/\alpha \cdot ((E - q \cdot V_p)/\epsilon)^\alpha), \quad (1)$$

where N is the normalization, V_p is the plasma potential, taking into account the shift induced in the zero energy position, ϵ is related to the mean energy of the ions, and α is a parameter describing how steep is the high energy tail of the distribution ($\alpha = 1$ is the standard Maxwellian thermal distribution). From the fitted parameter values, the mean energy could be then easily calculated and compared.

III. RESULTS AND DISCUSSION

The first measurements were performed to analyze the neutral gas phase. Figure 2 shows the spectra of neutral fragments sampled by the spectrometer held at a position corresponding to the edge of the source, approximately aligned to the electrode plate side.

A flowrate of 20 sccm was set corresponding to a pressure in the main chamber that stayed stable, 20.3 ± 0.2 Pa, during the data acquisition. A radiofrequency discharge with a power level of 50 W was operated, and the gas-phase composition [Fig. 2(a)] was compared with the unperturbed gas flow [Fig. 2(b)]. A nice, clean spectrum of oxygen (O_2 at amu = 32 peak) is obtained in both cases with impurities (mainly water vapor and carbon dioxide desorbing inside the spectrometer) below a few percent of this peak. Their level is only slightly increased during the discharge, despite the much larger interactions with the surfaces. The signal of the ^{18}O isotope (inferred from the amu = 34 peak, which has little contamination) agrees well with the natural abundance, confirming the uniform sensitivity of the instrument. It is also clear that the flux of atomic oxygen and, thus, the level of dissociation in the plasma gas phase are quite small at this level of radiofrequency power. The most interesting feature of such discharges lies in their charged particle content. This led to the core of our investigation, devoted to the measure of the density and energy distribution of the ions produced in the plasma state. Figures 3 and 4 display, respectively, the mass and the energy spectrum of ions in a typical discharge. The EQP spectrometer has a system of about twenty electrodes/lenses to perform ion extraction and analysis from the plasma state through the orifice. A couple of them, named Extractor and Lens-1, located just after the orifice, is crucial to ensure ions entering the spectrometer are collected without causing additional ionizations during their delivery to the detector.

Although a detailed discussion of the tuning procedure, as recommended by the manufacturer, is outside our aims, we recall that the adjustment to ensure a proper tuning of the ion focusing and the reduction of chromatic aberrations were performed whenever the plasma conditions (pressure and power level) have been changed. We also checked that tuning was optimal for the whole ion energy

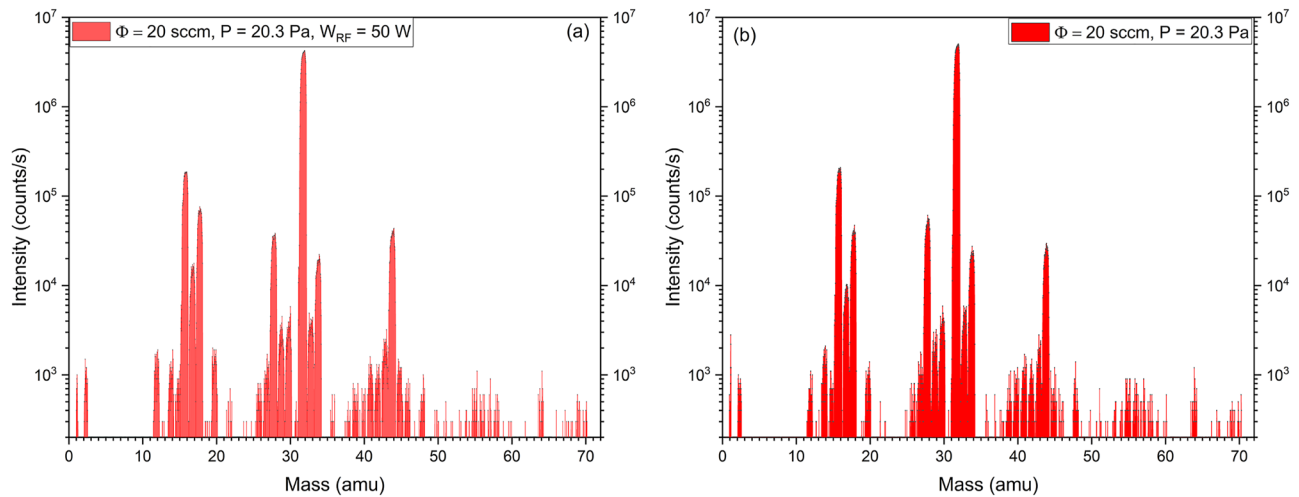


FIG. 2. The neutral mass spectrum of the chamber gas phase in an oxygen flow with (a) and without plasma (b). Signal above 70 amu was negligible and cut. ($\Phi = 20$ sccm, $P = 20.3$ Pa, $W_{RF} = 50$ W, electron impact energy 70 eV).

range that was observed from that selected plasma state. In particular, we cared to choose conditions to reduce the acceptance angle of ions in order to collect ions directly from the plasma facing the orifice.⁹ Ion mass spectra are collected at an energy corresponding to the maximum of the spectra.

The scan shows that the dominance of the O_2^+ ion was produced by direct electron impact ionization of the oxygen molecule. Some other ions (notably H_2O^+ , H_3O^+ , CO_2^+ , NO^+ at $M = 18/19/44/30$) are produced, possibly by charge exchange reactions, from impurities in the spectrometer or in the main chamber. The other interesting ion is the atomic oxygen one O^+ that could be produced by electron impact either by dissociative ionization of the parent

molecule or by direct ionization of a neutral oxygen atom, obviously coming from a previous dissociated molecule. In both cases, its abundance, roughly 1.3% in the displayed spectrum, reflects the dissociation induced by the plasma and its reactivity to any exposed material surface. As for the energy spectrum shown in Fig. 4 for molecular oxygen ions, we indeed observe both the shift and the broadening of the distribution. A similar shape was also observed also for the atomic oxygen ions energy distribution; however, because of its lower intensity, its details were obscured by larger noise. A fit using Eq. (1) yields as the best parameters $\varepsilon = 2.23 \pm 0.03$ eV and $\alpha = 2.18 \pm 0.06$. The average energy could be calculated and results $\langle E \rangle = 2.26$ eV with $T_e = 1.51$ eV. The

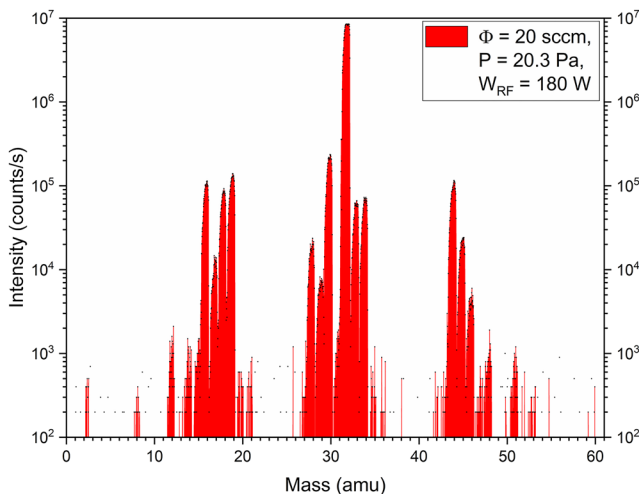


FIG. 3. The positively charged ion mass spectrum of the plasma gas phase in an oxygen radiofrequency discharge ($\Phi = 20$ sccm, $P = 20.3$ Pa, $W_{RF} = 180$ W). Signal above 60 amu was negligible and cut.

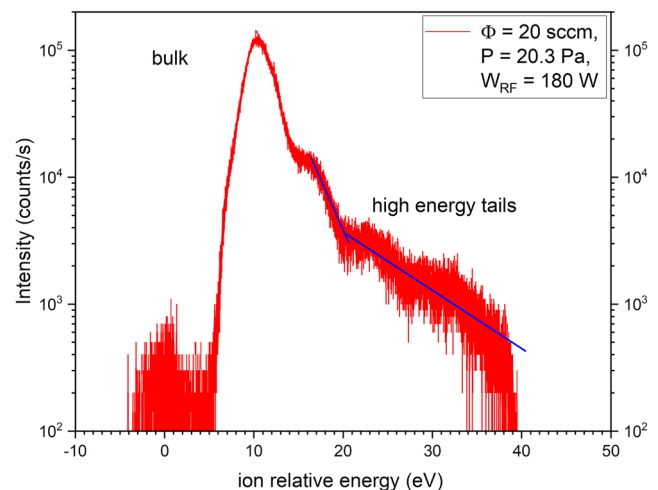


FIG. 4. The energy spectrum of the plasma molecular oxygen ions collected from the gas phase in an oxygen radiofrequency discharge ($\Phi = 20$ sccm, $P = 20.3$ Pa, $W_{RF} = 180$ W).

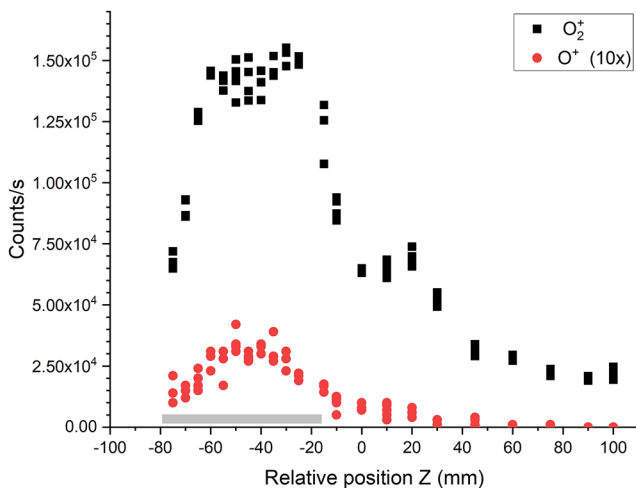


FIG. 5. Oxygen ions density profiles as a function of the position along the axis of the cylindrical vacuum chamber. The position corresponding to the plate electrode is also indicated.

distribution is then quite close to the Druyvestein energy distribution.¹³ The estimated plasma potential was $V_p = 8.71 \pm 0.02$ V. Besides the bulk distribution, the spectrum shows also two high energy tails, somewhat linear in the semilog-plot of Fig. 4. They could be fitted with functions having α of the order of one, indicating a Maxwellian tail of high energy ions, although with small populations ($E > 8$ and 14 eV, respectively).

Having discussed the potentiality of the analysis, we briefly discuss some results. Figure 5 shows the intensity of the molecular and atomic oxygen ion signals as a function of the position along the cylindrical vacuum chamber axis. Unsurprisingly, both profiles peak in the region corresponding to the electrode plate.

The two profiles also agree very well. An almost uniform plasma density is observed for roughly 3.5 cm, approximately within the plate interior. A sharp drop in density is observed at a location corresponding to the plate edge, as well as upstream. Downstream, however, a gentle profile extends up to the vacuum chamber wall, indicating that a diffused plasma fills the whole vacuum chamber. Figure 6 shows the intensity of the molecular oxygen ion signal as a function of the radiofrequency power level. After a somewhat linear increase at power slightly larger than the breakdown one (here at a mere $W = 3$ W), the ion density appears to saturate. At larger power levels ($W > 200$ W), a strong, almost exponential growth indicates a transition to a fully inductive coupling of the discharge.¹⁴

A similar analysis could be performed by measuring the energy distribution function at different locations, radiofrequency power levels, or oxygen pressures. In any case, a fit using Eq. (1) allows us to collect the relevant plasma parameters to be compared. As a glimpse of its utility, we display, in Fig. 7, the spatial distribution of the plasma potential along the chamber axis. The nice precision of our data allows us to appreciate the slight, almost linear profile, corresponding to a weak, axial electric field in the device, extending also inside the plate electrode interior. Finally, we present, in Fig. 8, the ion energy distribution measured by slowly decreasing the pressure

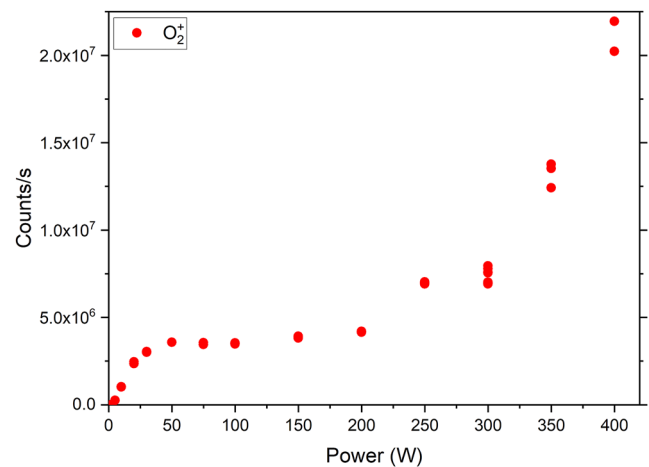


FIG. 6. Oxygen ion intensity signal as a function of the radiofrequency power.

level during a discharge, as the ion density and energy distribution rearranges themselves to the changing neutral oxygen density. The main aim of this investigation was to search for plasma conditions allowing a flow of energetic ions that could be collected by a flat material exposed to the discharge, as discussed previously. This could be accomplished by substituting the orifice plate surface of the mass-spectrometer (which is grounded in our experiments) with a grounded sample holder plate, actually simply a disk held at a fixed position on the cylinder axis. Positive plasma potentials result in ions being accelerated toward the plate, as it happens to those collected through the orifice in our spectrometer. Although some tens eV can be reached starting from the discharges discussed insofar, thanks to plasma potential of about 10 V and some high energy ion tails, a substantially stronger effect could be achieved by reducing pressure below 1 Pa. Here, bulk ion energies peaking between 30 and 70 eV

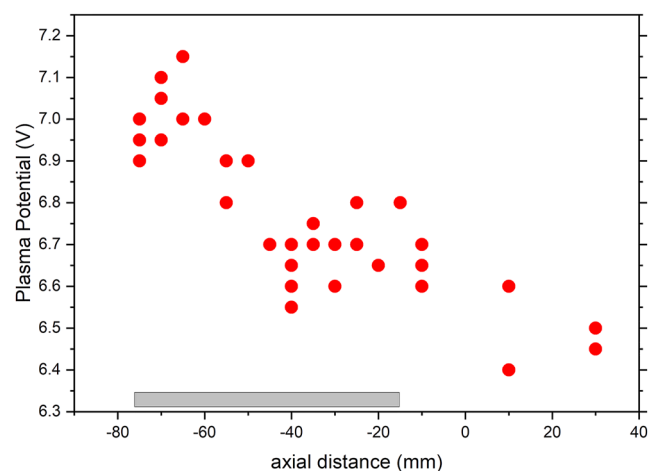


FIG. 7. Plasma potential obtained from Eq. (1) fit of the ion energy distribution along the cylindrical vacuum chamber. The location of the plate electrode is also indicated.

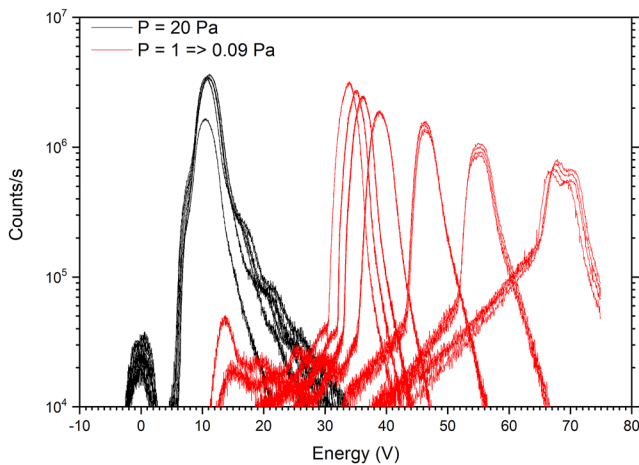


FIG. 8. Oxygen ion energy distributions recorded at different pressures of the neutrals during the RF discharge, at a position corresponding to the plate electrode edge. Different repetitions are superimposed to show the effect arising from discharge evolution.

have been observed, although with a reduced overall density. At the minimum experimented pressure of $P = 0.09$ Pa, a plasma potential of $V_p = 65$ V was observed, with tails at energies up to 75 eV, which was the limit set in our experiments. This demonstrates that plasma processing with high energetic ion fluxes can be accomplished in our device by choosing suitable operating conditions. Future work will be performed to evaluate the prospect it opens to several plasma functionalizations, the first being the formation of nanostructured polymer surfaces.²

IV. SUMMARY AND CONCLUSIONS

We have studied oxygen radiofrequency discharges by means of mass spectroscopy of the charged species, directly sampling the plasma gas phase at different locations. We were able to measure the composition as well as the density of the positive ions in the plasma, as a function of power level. We also measured the ion energy distributions, which have been analyzed to extract significant physical parameters of the plasma state, such as the mean electron energy and the plasma potential. Since our aim was to obtain a plasma state that could deliver a sustained flow of high energy oxygen ions, we identified promising discharges that could be reached by decreasing the neutral pressure below 0.1 Pa. This input will be applied to study the

polymer texturing and deposition processes in plasmas under the effect of such ion flux.

ACKNOWLEDGMENTS

We are pleased to acknowledge support of our present and past technical staff at the PlasmaPrometeo Center.

AUTHOR DECLARATIONS

Conflict of Interest

The authors have no conflicts to disclose.

Author Contributions

Ruggero Barni: Investigation (lead); Writing – original draft (lead); Writing – review & editing (lead). **Matteo Daghetta:** Validation (supporting); Writing – review & editing (supporting). **Cecilia Piferi:** Writing – review & editing (supporting). **Claudia Riccardi:** Conceptualization (lead); Project administration (lead); Writing – original draft (equal); Writing – review & editing (equal).

DATA AVAILABILITY

The data that support the findings of this study are available from the corresponding author upon reasonable request.

REFERENCES

- H. Biederman, *Plasma Polymer Films* (Imperial College Press, London UK, 2004).
- C. Piferi, K. Bazaka, D. L. D'Aversa, R. Di Girolamo, C. De Rosa, H. E. Roman, C. Riccardi, and I. Levchenko, *Adv. Mater. Interfaces* **8**, 2100724 (2021).
- E. C. Dell'Orto, S. Caldirola, A. Sassella, V. Morandi, and C. Riccardi, *Appl. Surf. Sci.* **425**, 407 (2017).
- M. Qu, Z. Cheng, Z. Sun, D. Chen, J. Yu, and J. Chen, *Process Saf. Environ. Prot.* **153**, 139 (2021).
- R. Barni, S. Zanini, and C. Riccardi, *Adv. Phys. Chem.* **2012**, 205380.
- R. Barni, S. Zanini, and C. Riccardi, *Vacuum* **82**, 217 (2007).
- M. Weiler, K. Lang, E. Li, and J. Robertson, *Appl. Phys. Lett.* **72**, 1314 (1998).
- M. R. Alexander, F. R. Jones, and R. D. Short, *J. Phys. Chem. B* **101**, 3614 (1997).
- S. Caldirola, R. Barni, H. E. Roman, and C. Riccardi, *J. Vac. Sci. Technol., A* **33**, 061306 (2015).
- C. Riccardi, R. Barni, and M. Fontanesi, *J. Appl. Phys.* **90**, 3735 (2001).
- V. A. Godyak and B. M. Alexandrovich, *J. Appl. Phys.* **118**, 233302 (2015).
- A. Schwabedissen, E. C. Benck, and J. R. Roberts, *Phys. Rev. E* **55**, 3450 (1997).
- V. A. Godyak and V. I. Kolobov, *Phys. Rev. Lett.* **81**, 369 (1998).
- F. Crocco, A. Quintini, R. Barni, and C. Riccardi, *High Temp. Mater. Process.* **14**, 119 (2010).